

Selective targeting of the IL23 pathway: Generation and characterization of a novel high- affinity humanized anti-IL23A antibody

Sanjaya Singh^{1,*}, Rachel R Kroe-Barrett¹, Keith A Canada^{1,†}, Xiang Zhu^{1,‡}, Eliud Sepulveda¹, Helen Wu¹, Yaqin He^{1,§}, Ernest L Raymond², Jennifer Ahlberg¹, Lee E Frego¹, Laura M Amodeo¹, Katrina M Catron^{1,#}, David H Presky¹, and Jeffrey H Hanke³

¹Department of Biotherapeutics Research; Boehringer Ingelheim Pharmaceuticals Inc.; Ridgefield, CT USA; ²Department of Immunology; Boehringer Ingelheim Pharmaceuticals Inc.; Ridgefield, CT USA; ³Global Head of Biotherapeutics Research; Boehringer Ingelheim Pharmaceuticals Inc.; Ridgefield, CT USA

Current affiliations: [†]Intrexon; Blacksburg, VA USA; [‡]Shanghai Huaota Biopharma; Shanghai, China; [§]Novartis; Cambridge, MA USA; [#]Middlebury, CT USA

Keywords: BI 655066, biophysical assessment, pharmacokinetic profile, humanization, immunogen design

Abbreviations: IL23, Interleukin-23; Th17, T helper 17 cells; IL12, Interleukin 12; IL23R, IL23 receptor; IL12RB1, IL12 receptor subunit beta 1; JAK2, Janus kinase 2; tyk2, tyrosine kinase 2; CDRs, complementarity-determining regions; V, variable; SPR, surface plasmon resonance; V_H, variable heavy; C_H, constant region; V_K, variable kappa; G, glycine; F, phenylalanine; Y, tyrosine; C_K, constant kappa; PK, pharmacokinetic; ADCC, antibody-dependent cell-mediated cytotoxicity; SEC, size-exclusion chromatography; AUC, analytical ultracentrifugation; HCLF, high concentration liquid formulation; UV, ultraviolet; EOF, electro-osmotic flow; DMF, dimethylformamide; GAHA, goat anti-human IgG gamma antibody; PBS, phosphate-buffered saline; RU, resonance units; ESI, electrospray ionization; CCG, Chemical Computing Group

Herein, we describe the generation and characterization of BI 655066, a novel, highly potent neutralizing anti-interleukin-23 (IL23) monoclonal antibody in clinical development for autoimmune conditions, including psoriasis and Crohn's disease. IL23 is a key driver of the differentiation, maintenance, and activity of a number of immune cell subsets, including T helper 17 (Th17) cells, which are believed to mediate the pathogenesis of several immune-mediated disorders. Thus, IL23 neutralization is an attractive therapeutic approach. Designing an antibody for clinical activity and convenience for the patient requires certain properties, such as high affinity, specificity, and solubility. These properties were achieved by directed design of the immunization, lead identification, and humanization procedures. Favorable substance and pharmacokinetic properties were established by biophysical assessments and studies in cynomolgus monkeys.

Introduction

There is strong evidence that the interleukin (IL)23/IL17 axis plays an important role in the development of chronic inflammation, and genetic studies have revealed a potential link between the IL23 receptor (IL23R) or its ligand and several inflammatory diseases, including psoriasis, inflammatory bowel disease, and graft-versus-host disease.^{1–6} Indeed, recent clinical studies of monoclonal antibodies targeting IL17A and IL23 have demonstrated significant efficacy in psoriasis, e.g., secukinumab, guselkumab, and tildrakizumab in Phase 3 studies; MEDI-2070 in Phase 1 studies.⁷ In addition, the monoclonal antibody

ustekinumab (CNTO-1275), which targets both IL23 and IL12 through their common p40 subunit, has demonstrated efficacy in psoriasis and other inflammatory conditions.⁷

IL23 plays a crucial role in the induction and function of pathogenic effector Th17 cells.^{8,9} While cytokines such as IL6 and TGF- β 1 can promote the differentiation of ROR γ t+ Th17 cells from naïve CD4+ T cells, IL23 is required for the full inflammatory function of these cells.^{10,11} In addition, the binding of IL23 to its receptor on activated ROR γ t+ Th17 cells induces further expression of the IL23 receptor (IL23R), thus providing a feed-forward loop for the maintenance and propagation of these cells.¹¹ Innate immune cells can also respond to

© Sanjaya Singh, Rachel R Kroe-Barrett, Keith A Canada, Xiang Zhu, Eliud Sepulveda, Helen Wu, Yaqin He, Ernest L Raymond, Jennifer Ahlberg, Lee E Frego, Laura M Amodeo, Katrina M Catron, David H Presky, and Jeffrey H Hanke

*Correspondence to: Sanjaya Singh; Email: Sanjaya.singh@boehringer-ingelheim.com

Submitted: 01/20/2015; Revised: 03/16/2015; Accepted: 03/18/2015

<http://dx.doi.org/10.1080/19420862.2015.1032491>

This is an Open Access article distributed under the terms of the Creative Commons Attribution-Non-Commercial License (<http://creativecommons.org/licenses/by-nc/3.0/>), which permits unrestricted non-commercial use, distribution, and reproduction in any medium, provided the original work is properly cited. The moral rights of the named author(s) have been asserted.

IL23 in concert with other cytokines to induce effector functions in vitro and in vivo.² For example, IL1 and IL23 are important for inducing ILC3 cells, which are known to be increased in psoriasis.^{12,13}

IL23 is a heterodimeric cytokine composed of 2 disulfide-linked subunits: a soluble p40 subunit and a tetra-helical bundle p19 subunit. The p40 subunit also associates with a p35 subunit to form the pro-inflammatory molecule IL12, and forms a homo-dimeric p40 that acts as a natural antagonist for both IL23 and IL12.¹⁴⁻¹⁸ IL23R forms a complex with the IL12 receptor subunit beta 1 (IL12RB1), and the p19 subunit of IL23 binds IL23R and the p40 subunit binds IL12RB1. Signaling through IL23R induces Janus kinase 2 (JAK2) and tyrosine kinase 2 (tyk2) phosphorylation, which activate STAT3, leading to the upregulation of ROR γ t, and subsequent increases in the inflammatory cytokines IL17 and IL22.¹⁹⁻²²

In this report, we describe the generation, humanization, and characterization of a novel anti-IL23 monoclonal antibody, BI 655066, that is currently in Phase 2 clinical trials for psoriasis, Crohn's disease and other indications.²³ Key design criteria included selectivity for the p19 over the p40 subunit, high affinity to overcome the high-affinity binding of IL23 to IL23R, the ability to maintain target coverage with administration once monthly or less frequently, and favorable biophysical properties.²⁴

Results

Immunization and selection of candidate murine antibodies

Toward the goal of generating a high-affinity antibody specific for the p19 subunit of IL23, pilot immunizations were performed using commercial baculovirus-derived recombinant human IL23. These immunizations revealed that the p40 subunit was immuno-dominant, with only low-affinity (single digit nM) antibodies selective for the p19 subunit being generated (data not shown). To minimize the immuno-dominance of the p40 subunit, we performed the immunizations with a hybrid mouse p40/human p19 recombinant cytokine. Unlike commercially available IL23, which is produced using linkers between the p40 and p19 subunits, we expressed the hybrid cytokine in mammalian cells as individual p40 and p19 subunits without linkers, similar to the native cytokine structure. The functional activity of the hybrid IL23, determined by its ability to induce IL17 production in mouse splenocytes, was similar to that of human IL23 released from lipopolysaccharide-stimulated THP-1 cells (data not shown). To select for functionally relevant antibodies, mammalian expressed human recombinant IL23 (with minimal use of linkers or tags) was used for screening and testing candidate antibodies. This recombinant form of human IL23 was equipotent compared to naturally expressed THP-1 cell-derived human IL23 as well.

Antibodies were selected based on their high-affinity binding to recombinant human IL23, assessed using Biolayer interferometry (Fortebio Octet), and their potency for inhibition of an EC80 concentration of human IL23-induced IL17 production in

mouse splenocytes. To ensure accurate measurements of K_d and IC50 endpoints in binding and functional assays, the antibodies were purified from the hybridoma culture supernatants prior to testing. This immunization and selection approach yielded antibodies to the human p19 subunit, with K_d measurements in the pM range and potent functional inhibition of human IL23-induced IL17 (Table 1). To ensure that the antibodies had minimal sequence liabilities in their complementarity-determining regions (CDRs) that could affect their manufacturability, they were cloned and sequenced, and the sequences were analyzed for potential deamidation sites, iso-aspartic isomerization hot spots, atypical glycosylation sites, and undesirable CDR composition (i.e., high hydrophobic or charged amino acid content). Sequence analysis of the mouse antibodies showed good diversity, indicating a robust immune response to the p19 subunit. The CDRs and potential deamidation and aspartate isomerization sequence liabilities of the top 5 candidates are shown in Table 2. Overall, these antibodies had a minimal number of potential deamidation and aspartate isomerization sequence liabilities. 6B8 was selected as the top anti-IL23 antibody based on assessment of the full data set, including affinity, functional potency and sequence, aligned with the lead finding strategy.

Characterization and selection of the top anti-IL23A antibody

To ensure that the correct sequences were recovered from the hybridoma, and that the cloned variable (V) genes maintained their affinity when grafted to human Fc, we generated chimeric antibodies. The chimeric antibodies were fully characterized for binding and function to ensure that their properties remained unchanged. The binding affinity of mouse 6B8 and recombinant chimeric 6B8 for human IL23 protein, as measured by surface plasmon resonance (SPR), was 25 and < 10 pM, respectively, confirming that the correct sequence was cloned from the hybridoma. The higher binding affinity

Table 1. Binding affinity and functional inhibition (IC50) of antibodies purified from representative hybridomas generated in the hybrid immunization campaign. Several antibodies with < 10 picomolar affinity and high potency to block IL23 induced IL17 production in mouse splenocytes assay were identified

Hybridoma	Inhibition of IL23 induced IL17	
	K_d IL23 (pM)	production in mouse splenocytes (IC50, pM)
18C4	<10	56
18E5	<10	< 13
18D3	<10	< 13
20E8	640	499
22E2	1020	102
24A5	22	131
15C11	26	197
43F5	35	2000
27G8	27	235
31H9	12	960
9D12	< 10	188
6B8	< 10	8
26F7	28	9
34G3	33	8

Table 2. Anti-IL23A monoclonal antibody CDRs (Chothia) and in silico-predicted liabilities. Predicted deamidation-prone asparagines (blue) and isomerization-prone aspartates (red) are shown. Clone 6B8 had no predicted liability in Kabat CDRs and one deamidation site when Chothia or Chemical Computing Group (CCG) CDR definition was used

Name	H-CDR1	H-CDR2	H-CDR3	Deamidation	Aspartate Isomerization
6B8	GNTFTDQTIH	YIYPRDDSPKYENFKG	PDRSGYAWFIY	1	0
18E5	GYTFTRYLIH	YINPYNDGTKYNEKFKG	NWDLDY	1	1
26F7	GYTFTDYMMN	DFNHNNDEVITYNPKFKG	GLRGYYAMDY	3	0
34G3	GYSFTDYNMN	VIIPNYGFTSYNQNFKG	DGGILLWYLDV	0	1
15C11	GYTFTDYMMN	VIIPYNGGTSYNQKFKG	DGHRWYFDV	1	1

Name	L-CDR1	L-CDR2	L-CDR3	Deamidation	Aspartate Isomerization
6B8	KASRDVAIAVA	WASTRHT	HQYSSYPFT	0	0
18E5	RASQISDYLY	FASQIS	QNGHSFPFT	1	0
26F7	RASKSVRFSDYFYM	LASNLES	QNSRELPTY	1	0
34G3	RSSQSLVHSNGNTYLH	KVSNRFS	SQSTHVPYT	2	0
15C11	RSSQSLVHSNGNTYLH	KVSNRFS	SQSTHVPYT	2	0

of the chimeric antibody compared to the fully murine one may have been due to flexibility differences in the human and mouse IgG1 constant domain. To confirm specificity, the antibodies were screened for their ability to bind human IL12. Neither antibody bound IL12 up to 1.2 μ M, the highest concentration tested (data not shown). Using an Fc-fused IL23 receptor, it was determined that recombinant chimeric antibody 6B8 efficiently blocks binding of IL23 to its receptor (Fig. S1). The murine and chimeric 6B8 antibodies also showed similar potencies to inhibit human IL23-induced IL17 production in mouse splenocytes, with IC50s of 4 and 5 pM, respectively.

Humanization and sequence optimization of clone 6B8

To humanize the 6B8 antibody, we selected the most homologous human germ-line antibody sequences, IGKV1-27*0, KJ2 for the light chain and IGHV1-69*08, HJ4 for the heavy chain (Fig. 1a). It is known that CDR grafting alone is not sufficient to maintain an antibody's full binding properties, and that framework residues are critical for maintaining the proper CDR conformations for binding affinity.^{25,26} To evaluate the framework residue requirements for 6B8 functionality, a library of variants was generated that mostly focused on residues flanking the CDRs, in which each residue being considered was altered between the human and murine residue (Fig. 1).



Figure 1. 6B8 Optimization design (a, light chain; b, heavy chain). CDRs as per the CCG definition are underlined. Amino acids different from the 6B8 hit are colored red if divergent or orange if similar. ~: Sites where binary mutations (mouse and human) were included in the library. ≈: The site mutated to G, F, or Y to eliminate a potential deamidation motif, N27T28 (colored aqua).

To humanize the light chain, in addition to grafting the CDRs, the selected human germ-line framework residues 3, 13, 48, 49, 60, 68, 83, 85, 87, and 100 were altered between the human and murine residue. These residues were selected based on their proximity to the CDRs. All others were changed to human. If these residues had not worked we would have considered additional residues in further iterations. Working in smaller libraries minimizes the total number of clones that need to be evaluated and keeps the process efficient. The variable heavy (V_H) of 6B8 fused with human constant region 1 (C_{H1}) was used as the heavy chain in expressing the light chain variants as Fabs. The variable kappa (V_K) chain was optimized in the context of the parental V_H chain to lower the possibility of functional and epitope drift.²⁷ Given that each position can contain either the human or mouse residue, and that there are 10 positions that are being altered, a total of 1024 variations are possible for the light chain. Approximately 3000 independent clones were

evaluated by an ELISA for IL23 binding to sufficiently cover the diversity in the library. A chimeric 6B8 Fab with murine variable regions grafted to human constant regions was produced to serve as a positive control for screening and measuring the maintenance of affinity and potency. A key design attribute of our Fab expression vector system was the removal of the natural inter-chain (heavy and light chain) disulfide bond by Cys-Ser mutation, which enabled us to screen for stable Fabs with innate V_H and V_K pairing.

Approximately 100 candidate hits with a binding affinity for IL23 greater than or equal to the true chimeric 6B8 Fab were sequenced and ranked to identify those with the lowest number of retained mouse residues in the framework regions and the most favorable EpiVax (in silico immunogenicity prediction) scores. The hits were confirmed by the ELISA for IL23 binding and ranked according to k_d measured by SPR. The k_d s ranged from 6.0×10^{-4} to $1.8 \times 10^{-5} \text{ s}^{-1}$. The sequence information

	1	10	20	30	40
>Vk Design	DI~MTQSPSSLS~SVGDRVTITC <u>KASRDVAIAVAWYQQK</u> P				
VK 65	Q	A			
VK 66	Q	A			
VK 78	Q	A			
	41	50	60	70	80
>Vk Design	GKVPKLL~~ <u>WASTRHTGVP</u> ~RFSGSGS~TDFTLTISSLQP				
VK 65		LF	D	G	
VK 66		IY	S	R	
VK 78		LF	D	R	
	81	90	100		
>Vk Design	ED~A~Y~ <u>CHQYSSYPFTFG</u> ~GTKLEIK				
VK 66	L D Y		Q		
VK 67	V D F		S		
VK 78	L D Y		S		

Figure 2. Top-selected optimized V_K sequences. Mouse germ-line residues are shown in black, and human germ-line residues are in blue. The V_K sequences 65, 66, and 78 were 96, 93, and 94 percent identical to the human germ-line genes **IGKV1-27*01,KJ2**), respectively, and had corresponding EpiVax scores of -40, -43, and -38.

of the top optimized V_Ks selected for pairing with the humanized heavy chain (described below) is shown in **Figure 2**.

To humanize the heavy chain, 11 V_H framework positions (20, 24, 37, 38, 40, 48, 67, 68, 70, 95, and 98) mostly based on their proximity to the CDRs were evaluated. In addition, one potential deamidation site (“NT”) in H-CDR1 (Chothia), N27, was selected for mutagenesis to a glycine (G), phenylalanine (F) or tyrosine (Y) (common human germ-line residues at this position) to determine if the potential deamidation site could be removed. The V_K of 6B8 fused with human constant kappa (C_K) was used as the light chain in generating Fabs, and the library was screened similarly to the V_K chain variants. The hits were ranked by the ELISA for IL23 binding and by k_d determined by SPR (values ranged from 1.0×10^{-6} to $3.7 \times 10^{-4} \text{ s}^{-1}$). The confirmed hits were further ranked to

identify those with the lowest number of retained mouse residues in the framework regions and most favorable EpiVax in silico immunogenicity prediction scores. The sequence information for the top 4 optimized V_Hs selected for IgG conversion is presented in **Figure 3**.

The top 4 optimized V_H chains and 3 V_K chains were subcloned into pcDNA3.1 vectors containing genomic IgG1 expression cassettes, using standard PCR restriction enzyme-based cloning techniques. The matrix of 12 optimized IgGs was expressed transiently in HEK293F cells. **Table 3** shows the K_ds of each of the 12 optimized IgGs, which ranged from 107 pM to <math><10 \text{ pM}</math> (limit of detection). From these data, the top 4 IgGs, BI 655066-BI 655069 (**Table 3**) were selected for further profiling based on their binding affinity and potency and the percentage of human residues in the final molecule.

	1	10	20	30	40
>VH Design	QVQLVQSGAEVKKPGSSVK~SCK~SG~TFTDQTIHW~Q~				
VH 02				V A Y	MR A
VH 05				V A F	VR A
VH 36				T A G	VR R
VH 65				V A G	VR A
		41	50	60	70 80
>VH Design	PGQGLEW~GYIYPRDDSPKYNENFKG~T~TADKSTSTAY				
VH 02		I		KV I	
VH 05		M		KV L	
VH 36		M		RV I	
VH 65		M		RV L	
		81	90	100	110
>VH Design	MELSSLRSEDTAVY~CA~PDRSGYAWFIYWGQGLVTVSS				
VH 02			Y I		
VH 05			Y I		
VH 36			Y I		
VH 65			F R		

Figure 3. Top selected optimized V_H sequences. Mouse germ-line residues are shown in black, and human germ-line residues are in blue. Amino acids changed to remove a deamidation site are shown in green. V_H sequences 02, 05, 36 and 65 were 95, 96, 96, and 98 percent identical to the human germ-line genes (IGHV1-69*08, HJ4), respectively, and had corresponding EpiVax scores of -17, -38, -17, and -34.

Table 3. Binding affinities and EpiVax scores for IgGs sequence-optimized to human IL23 Clinical candidate, BI 655066, has < 10 picomolar affinity for IL23 and highly favorable EpiVax score indicating low predicted immunogenicity in humans

IgG	K _d for human IL23 (pM)	EpiVax (VK)	EpiVax (VH)	BI Name
VH 02-Vk65	15	-40	-17	BI 655068
VH 05-Vk65	<10	-40	-38	BI 655067
VH 36-Vk65	96	-40	-17	—
VH 65-Vk65	107	-40	-34	—
VH 02-Vk66	<10	-43	-17	BI 655066
VH 05-Vk66	36	-43	-38	BI 655069
VH 36-Vk66	<10	-43	-17	—
VH 65-Vk66	<10	-43	-34	—
VH 02-Vk78	<10	-38	-17	—
VH 05-Vk78	13	-38	-38	—
VH 36-Vk78	<10	-38	-17	—
VH 65-Vk78	<10	-38	-34	—

Characterization of top antibodies

To select the final lead molecule, the following selection criteria were used: (1) cross-reactive binding to rodent and cynomolgus IL23 to enable preclinical pharmacokinetic (PK) and safety studies; (2) functional inhibition of IL23-induced IL17; (3) serum interference; (4) in vivo inhibition of IL23-induced cytokine induction and inflammation; (5) expression analysis; (6) biophysical property assessments; and (7) cynomolgus monkey PK studies.

To guide selection of the safety species, the antibodies were tested for their ability to bind cynomolgus and rodent IL23 by SPR. The K_ds for 2 of the top antibodies were beyond the limit of detection of the instrument for both human and cynomolgus IL23 (Table 4). This finding implies that the K_d was <10 picomolar. No binding to rodent IL23 was observed at concentrations up to 1.2 μM (data not shown). The antibodies' specificity for IL23 was confirmed, as no binding to human or cynomolgus IL12 was observed at concentrations up to 1.2 μM (data not shown).

After confirming binding affinity and selectivity, the antibodies were tested for inhibition of IL23-induced IL17 production in a mouse splenocyte assay using both THP-1 cell-derived human IL23 and recombinant cynomolgus IL23. IC50 values of 2 to 655 pM were found for the antibodies, indicating potent functional activity and cross-reactivity with cynomolgus IL23 (Table 4). A dose response curve for BI 655066 is shown in Figure S2, which indicates an IC50 value of approximately 2

pM. The antibodies were also titrated against both recombinant rat and mouse IL23 in the mouse splenocyte assay. The antibodies did not inhibit the IL17 production induced by either rodent molecule at concentrations up to 33 nM, indicating a lack of cross reactivity with each of these species (data not shown). This finding was consistent with the observation that neither rat nor mouse IL23 bound to the antibodies when tested in the SPR assay (data not shown). These data confirmed that the antibody was functional in the cynomolgus monkey, which could thus be used as the safety-testing species.

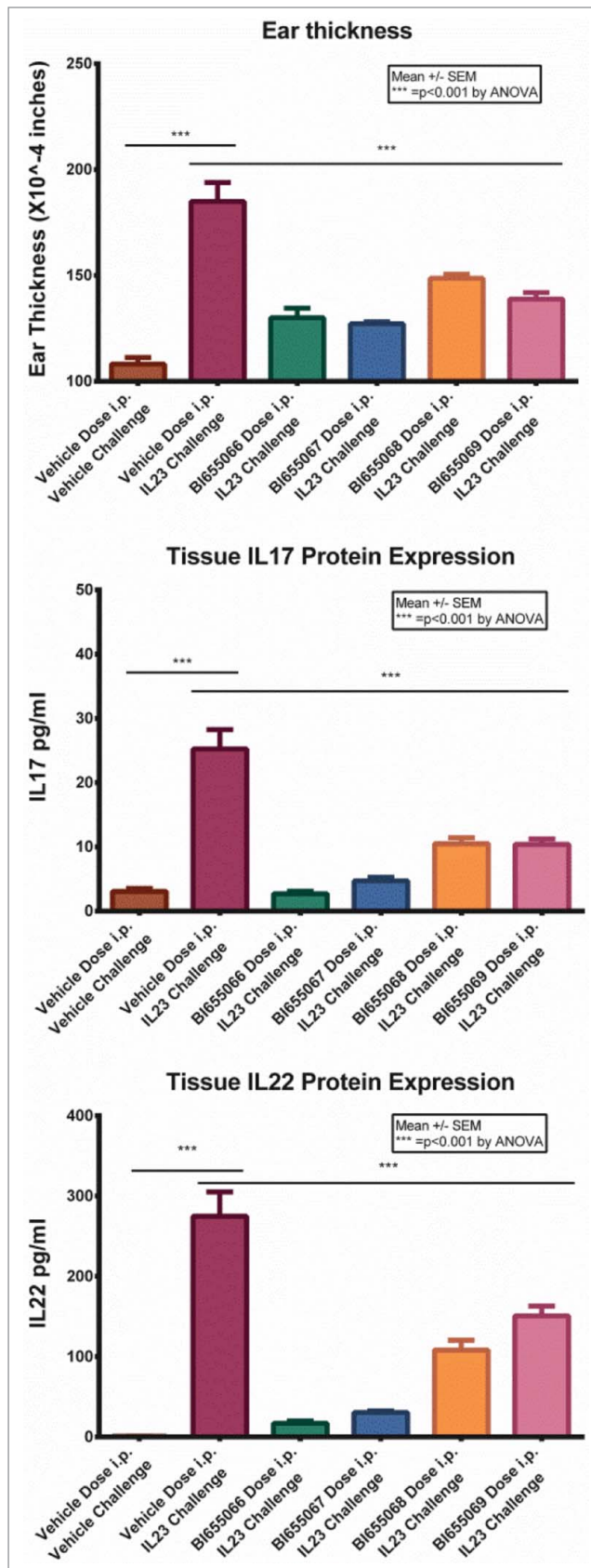
As a general measure of specificity, antibodies were analyzed for binding to human IL23 in the presence of 50% human serum to assess the potential for interference due to non-specific protein binding. The ratio of the on-rate in serum relative to buffer was <2 for each of the 4 antibodies, demonstrating that the antibodies did not weakly associate with serum proteins, and were specific for their target (Table 4).

To assess the antibodies' ability to block IL23 function in vivo, the antibodies were tested in a human IL23-induced model of skin inflammation. In this model, recombinant human IL23 was injected into the skin of the mouse ear for 4 consecutive days. One hour before the first dose of human IL23, the mice were given a single intraperitoneal (i.p.) dose of vehicle or 1 mg/kg antibody. Twenty-four hours after the last IL23 injection, the ear thickness was measured and ear tissue was harvested for IL17 and IL22 cytokine measurements by ELISA. Treatment with the anti-IL23 antibodies resulted in significant reductions of both the swelling response and the cytokine production induced by IL23 injection (Fig. 4). All four antibodies demonstrated significant inhibition of IL23 induced ear swelling and cytokine production.

To assess the expression and purification potential of the top antibodies, each was expressed as a stable pool in NS0 cells. The vector utilized for expression contained a human IgG1 Fc with 2 mutations (L234A and L235A), which limited the potential for antibody-dependent cell-mediated cytotoxicity (ADCC) effector function. This mutant Fc does not bind to CD32, and hence lacks the ADCC effector function.²⁸ Titers > 200 mg/L were achieved without optimization, with BI 655066 attaining a titer >300 mg/L (Table 5). The antibodies were subsequently purified using a Protein A affinity column followed by an ion-exchange column. The Protein A yield for each of the antibodies was 80%, indicating good recovery. Since protein expression and purification results are indicative of the overall stability and quality of an

Table 4. In vitro profile of 4 sequenced optimized variants. Clinical candidate, BI 655066, showed highest affinity and functional potency against human and cynomolgus IL23 induced IL17 production in the mouse splenocytes assay. To evaluate non-specific binding to irrelevant serum proteins an interference assay was performed demonstrating no change in the on-rate of the antibodies binding to IL23 in the presence of serum, indicating no non-specific binding

Parameter / Assay	BI 655066	BI 655067	BI 655068	BI 655069
K _d human IL23 (pM)	< 10	< 10	15	36
K _d cynomolgus IL23 (pM)	< 10	< 10	<10	16
Serum Interference [k _{on} (serum)/k _{on} (buffer)]	1.2	1.2	1.0	1.2
Inhibition of endogenous (THP-1 cell generated) human IL23-induced IL17 production (IC50, pM)	2	7	43	216
Inhibition of recombinant cynomolgus IL23-induced IL17 production (IC50, pM)	17	54	145	665



antibody, these data suggested that the selected antibodies were of high quality.

In addition to assessing the antibodies' purity and homogeneity using standard methods such as SDS-PAGE and analytical size-exclusion chromatography, we examined their homogeneity using analytical ultracentrifugation (AUC). AUC is a solution technique requiring no separation media or membranes that can lead to the loss of sample components due to protein/gel matrix interactions. In addition, AUC preparations can be analyzed using various solvent conditions, it is usually compatible with formulation buffers, and it covers a very wide range of molecular sizes.²⁹ Sedimentation velocity analysis of all the antibodies after the protein A step routinely revealed that they were ~98% monomers (Table 5).

Valence is a characteristic that can be of tremendous value in assessing liabilities in concentrating protein solutions.³⁰ Even though the valence of an antibody can be estimated from the amino acid sequence by summing the charge on each ionizable group, this method is not accurate, because various factors, including solvent type, concentration, pH, and temperature can affect the net valence of an antibody in solution. It was recently demonstrated that IgG1 molecules with experimentally determined valence values >+15 at pH 5 have the electrostatic repulsion necessary to achieve attractive solubility properties and high concentration liquid formulation (HCLF) with low viscosity.³¹ Our data have also shown that antibodies with a valence > +15 at pH 5.0 can achieve HCLF. Thus, the valence of each antibody at pH 5.0 was measured as an assessment of its solubility and the likelihood for low viscosity at high concentrations. The valence values are shown in Table 5. A solubility concentration test was also performed using 60 mM sodium citrate, 115 mM NaCl, pH 6.0 buffer to assess the potential challenges of concentrating the antibody and propensity for aggregation in concentrated form. The antibodies were concentrated to >100 mg/ml and assessed for monomer percentage by sedimentation velocity. Each antibody remained >96% monomers at this concentration without additional formulation (Table 5). To assess stability, the antibodies were evaluated for thermal stability by differential scanning calorimetry. The four antibodies had very similar unfolding profiles, melting as a single cooperative transition with a T_m of ~85°C.

Based on the combined data collected for the top 4 antibodies, BI 655066 was selected for further characterization as a prospective clinical candidate. This decision was driven by this antibody's high affinity, potency, selectivity, and favorable biophysical properties. Our experience with multiple antibodies has shown that expression in NS0 generally does not impact the intrinsic properties (as measured above) compared to CHO expression systems. As expected, binding studies revealed

Figure 4. IL23 was injected into the skin of the mouse ear every 24 h for 4 consecutive days. Mice were given a single intraperitoneal dose of vehicle or 1 mg/kg antibody 1 h before the first IL23 injection. Twenty-four hours after the last IL23 injection, the ear thickness was measured and ear tissue was harvested for IL17 and IL22 measurement by ELISA. Values are the mean +/- SEM. Statistical analysis by ANOVA.

Table 5. Biophysical and Manufacturability Profile. Optimized antibodies could be expressed in NS0 cells with ease, had high monomeric content, solubilized to over 100 mg/mL concentrations in citrate based buffer, measure valence over +17.8 and thermal stability was in the range of 84–85°C

Assessment	BI 655066	BI 655067	BI 655068	BI 655069
Stable Pool Titer	300 mg/L	217 mg/L	227 mg/L	221 mg/L
AUC (% monomer)	98%	98%	96%	98%
Valence	+ 20.4	+ 22.5	+ 17.8	+ 19.6
Solubility (% monomer)	99% at 108 mg/ml	98% at 105 mg/ml	96% at 115 mg/ml	98% at 120 mg/ml
Thermal Stability	85°C	85°C	84°C	85°C

comparable affinity of less than 10 pM for both the NS0 and CHO derived antibodies (Fig. S3). Similarly, other biophysical and stability parameters were comparable with only minor variations in glycosylation observed between NS0- and CHO-derived BI 655066 (Fig. S4).

Epitope mapping

To define the specificity of the binding site for BI 655066 on human IL23, mapping of the lead candidate was performed.³² BI 655066 was incubated with an equimolar amount of IL23 in deuterated buffer. IL23 protein alone served as the control. Differences in hydrogen/deuterium exchange between IL23 alone and IL23 with antibody present are indicative of solvent protection. The protection map (Fig. 5) and further refinements of the analysis showed significant protection of regions identified as amino acid residues 89 to 107 (IFTGEPSSLPDSPVGLHA) and amino acid residues 118 to 132 (PEGHHWETQQIPSL) on the p19 subunit of the IL23 heterodimer. This indicated that the lead bound to specific regions on the p19 subunit of the IL23 heterodimer. No exchange differences were seen in the p40

subunit of IL23 (data not shown), supporting the desired specificity of the antibody.

Pharmacokinetics in cynomolgus monkey

BI 655066 demonstrated favorable PK in cynomolgus monkeys following a single 1.0 mg/kg intravenous dose (Fig. 6, Table 6). A low mean systemic clearance (5.18 mL/d/kg) was observed, consistent with the reported values for other low-dose human IgG1 antibodies targeting soluble antigens.³³ The volume of distribution of BI 655066 in the monkeys was 88.3 mL/kg, suggesting that the distribution of BI 655066 was mainly confined to the intravascular space, which was also consistent with the volume of distribution for high-quality therapeutic IgG-based monoclonal antibodies targeted against soluble antigens. The bioavailability was estimated to be 70% by a cross-study comparison of single-dose subcutaneous vs. intravenous administration, and the mean C_{max} and T_{max} was 10.1 µg/mL and 2.1 days, respectively. The mean half-life following intravenous and subcutaneous administration ranged from 9 to 12 days, consistent with the reported half-life for high-quality therapeutic IgGs in monkeys (11 ± 2 days).³³

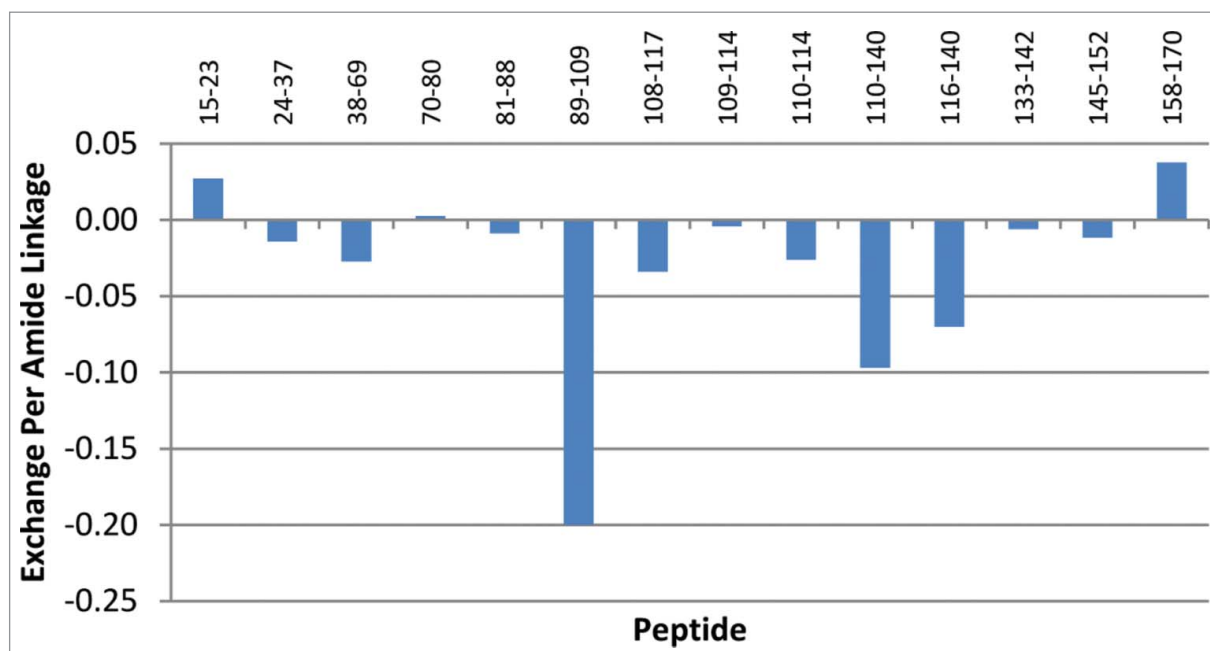


Figure 5. Hydrogen/Deuterium Exchange Mass Spectrometry. P19 peptides identified and their extents of exchange with BI 655066, as compared to control. All peptides showing exchange differences are found within the p19 subunit. The y-axis shows the calculated exchange normalized per amide.

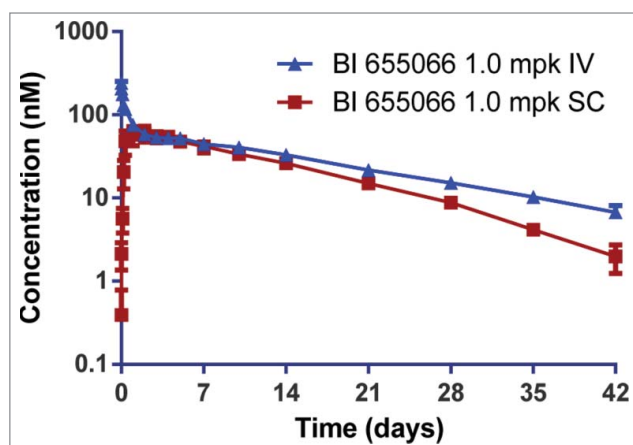


Figure 6. Pharmacokinetics of BI 655066 in cynomolgus monkeys following a single 1 mg/kg intravenous (IV) or subcutaneous (SC) dose. Serum concentrations were measured using an IL23-capture ELISA. Data are the mean \pm SD of three monkeys per dose route. Bioavailability was estimated to be $>70\%$, and the half-life (9–12 days) was similar after intravenous or subcutaneous administration.

Discussion

Here we describe the generation and characterization of a novel high-affinity humanized anti-IL23A antibody, BI 655066. This antibody selectively targets the p19 subunit of IL23 with a $K_D < 10$ pM and potently inhibits IL17 production in a mouse splenocyte assay. BI 655066 was selected and optimized to have excellent biophysical and PK properties as demonstrated by the ability to concentrate solutions to > 100 mg/ml and the observed 9–12 day half-life in cynomolgus monkeys. This antibody has successfully concluded Phase 2 clinical studies of patients with chronic plaque psoriasis, and is continuing to be evaluated in multiple other inflammatory diseases, including Crohn’s disease and ankylosing spondylitis.

Due to its important role in the induction and maintenance of autoimmunity, numerous efforts have been made to address the IL23/IL17 axis therapeutically.² Ustekinumab and briakinumab, which target the shared p40 subunit of IL23 and IL12, were evaluated for clinical use and ustekinumab has been approved for psoriasis and psoriatic arthritis.³⁴ Antibodies that target IL17A, IL17RA, and IL17A/IL17F (a shared motif) are now in clinical trials for a variety of autoimmune diseases, including psoriasis,

rheumatoid arthritis, Crohn’s disease, ankylosing spondylitis, and psoriatic arthritis.²

We focused on generation of a selective and potent antibody directed to the p19 subunit of IL23. This approach was favored over development of anti-p40 antibodies because it avoids effects on the IL12 cytokine axis (via p40). While agents that target the p40 subunit show robust clinical activity for some autoimmune diseases, it is not clear if direct modulation of the IL12 axis via p40 contributes to the efficacy or has potential risks related to IL12’s roles in tumor immune surveillance and in host defense against intracellular pathogens. Hence, selectivity for p19/IL23 could offer important differentiation in efficacy or safety. In addition, in contrast to directly antagonizing IL17 function, an IL23-blocking antibody should inhibit the development and propagation of pathogenic Th17 cells, leading to reductions in multiple pro-inflammatory cytokines associated with this cell type, such as IL17, IL21, and IL22.^{16,17,19,20,35} IL22 is particularly interesting, as it primarily affects the cells in barrier surfaces of the body, such as epithelia of the lung, gastrointestinal tract, and skin, and it has been suggested to be a driver of enthesitis pathogenesis.^{36,37}

BI 655066 potently binds to IL23 and blocks its binding to the IL23 receptor. The IL23R is highly responsive to its cognate ligand, and IL23 can elicit its response at very low concentrations.²⁴ Thus, a potent blocking antibody to IL23 is likely needed to inhibit this pathway effectively. In addition, less frequent dosing is a desirable factor in treating chronic diseases.³⁸ Therefore, the designed features of this therapeutic antibody included the potent inhibition of IL23 activity, a long half-life with sustained target coverage, low immunogenicity, and favorable biophysical properties.

Because initial antibody leads can dramatically influence the quality of a final lead antibody, we performed *in vivo* immunization using native paired (without linkers) p40/p19. A hybrid murine p40/human p19 form of IL23 was used to direct the immune response to the p19 subunit. We chose the approach of *in vivo* immunization and selection of antibodies over phage libraries because of the known potential challenges related to antibodies derived from phage-display libraries.³⁹ Most of the antibodies that are currently in Phase 3 clinical trials are either humanized or have been derived from transgenic animals.⁴⁰ Therefore, our strategy was to work under physiologically relevant conditions and to take advantage of the *in vivo* selection process to generate high-affinity antibodies.^{41,42}

Table 6. Noncompartmental pharmacokinetic parameters of BI 655066 in cynomolgus monkey. Pharmacokinetic parameters for BI 655066 in cynomolgus monkeys after a single 1 mg/kg intravenous or subcutaneous dose. Serum concentrations were measured using an IL23-capture ELISA. Pharmacokinetic parameters were determined by noncompartmental analysis. Data represent the mean \pm SD of three monkeys per dose route. AUCinf: area under the serum concentration-time curve from zero to infinity; CL: serum clearance; Vss: steady-state distribution volume; t1/2 half-life; C_{max}: maximum observed serum concentration; T_{max}: the time C_{max} was observed; F%: bioavailability

Dose (mg/kg)	Route	Animal/ group	AUCinf (ug·day/mL)	Clearance (mL/day/kg)	Vss (mL/kg)	t1/2 (day)	Cmax (ug/mL)	Tmax (day)	F%
1.0	i.v.	Mean	202	5.18	88.3	12.2	ND	ND	
		SD	33.5	0.8	3.12	2.28	ND	ND	
1.0	s.c.	Mean	142	ND	ND	9.15	10.1	2.11	70.4
		SD	33.3	ND	ND	1.87	3.14	1.84	16.5

ND = not determined.

Following the identification of high-affinity leads, our humanization approach was designed to maximize similarity to the human germ-line sequence, reduce iteration in selecting critical framework residues, and ensure the selection of optimal heavy and light chain pairs. This step was critical, as antidrug antibodies may neutralize therapeutic function, influence PK, and, in some cases, lead to severe adverse effects.⁴³ The identification of framework residues that are essential for maintaining affinity typically requires an iterative and somewhat unreliable approach to create, characterize, and correct, even when structure-based models are used.⁴⁴ Therefore, we used a library approach, in which each framework residue being considered was altered between the most homologous human germ-line sequence and the original murine sequence. A total of 21 framework amino acid residues in the heavy and light chains were tested, which resulted in a molecule with the desired properties. The removal of a deamidation site from the CDR H1 was also accomplished in this process by incorporating redundancy at the desired site.⁴⁵

As part of the selection process, the leads were analyzed for the percentage of human residues in the framework regions and for potential immunogenicity using the Treg adjusted scores from the EpiVax Epimatrix *in silico* immunogenicity prediction program. This approach yielded a favorable prediction of low to no immunogenicity for BI 655066 in humans. In addition, stabilization provided by the covalent interchain disulfide bond, normally present in the Fabs, may mask impairments in heavy and light chain pairing during the optimization process. Therefore, we removed this bond in the Fab expression vector used to generate the library during the engineering process to ensure that only optimally paired heavy and light chains that maintained their binding were selected for evaluation.

A critical element of our overall approach to identifying and selecting an attractive therapeutic antibody was the use of biophysical characterization early in the process.^{46,47} A detailed evaluation process was established under the premise that clinical success depends significantly on the inherent quality of the initial leads from the immunization and optimization processes.⁴⁸ In addition, the selected therapeutic molecule must be amenable to commercial scale-up and formulation. Key areas of analysis included aggregation, thermostability, valence, and turbidity profiles. Molecules with poor aggregation profiles can show activity loss, altered PK, and an increased risk of immunogenicity.⁴⁹⁻⁵¹ Thermostability, valence, and turbidity are indicators for *in vitro/in vivo* stability and solubility.⁵² Our results indicated that our lead candidates had attractive melting profiles, which is suggestive of potential long-term stability for our therapeutic product. As concentrations up to 150 mg/mL are often required for subcutaneous administration, properties such as valence, solubility, and turbidity provide early indications of the ease of development of a desirable HCLF.⁵³ BI 655066 meets these requirements, which allowed its development for subcutaneous administration in clinical studies.

Key factors that influence the PK of a molecule beyond the target-driven clearance include chemical stability, non-specific binding, immunogenicity and the efficiency of FcRn-mediated recycling.⁵⁴ The optimization of BI 655066 included assessments of molecule properties such as stability in whole blood (data not

shown), amino acid modification (i.e., deamidation), propensity for non-specific binding, *in silico* immunogenicity scores and ability to effectively interact with FcRn at pH 6.0 (data not shown). These assessments gave us confidence that BI 655066 would have a favorable PK profile, which we initially demonstrated in cynomolgus monkey and has now been validated in man.²³

In summary, using strategic approaches and tactically applying various biophysical assessment tools in our decision-making, we generated a highly potent humanized antibody with attractive properties for intervening in the IL23/IL17 axis.

Materials and Methods

Expression and purification of recombinant human IL23A, cynomolgus IL23A and endogenous IL23A

Suspended HEK293F cells were transfected with full-length p40 and N-terminally HIS-tagged p19 DNA using the TransIT-PRO system (Mirus Bio LLC). The transfected cells were incubated for 4 days, then the medium was harvested and applied to a Ni-NTA His-Bind Superflow column (Novagen) following the manufacturer's conditions. IL23 eluted from the Ni column was further purified by SEC. Cynomolgus IL23A was generated using the same method as described above for human. Culture supernatant from an activated human monocytic cell line THP-1 was used as a natural (endogenous) source of human IL23.⁵⁵

Generation of anti-IL23A antibodies

NMRI × C57/Bl6 mice were immunized with various forms of recombinant IL23. Hybridomas were generated by fusion with PAI myeloma cells using standard methods. Antibodies were purified from cultured hybridoma supernatants using Mab-SelectSuRe resin (GE Healthcare).⁵⁶ To identify the mouse anti-human IL23 IgGs with high affinity and specificity to human IL23, the purified antibodies were bound to human IL23 and human IL12 on an Octet QK system (ForteBio) equipped with streptavidin (SA) biosensor tips (ForteBio). Variable gene sequences were recovered from hybridomas using standard methods, and chimeric antibodies were generated to verify the characteristics of the recovered antibodies.⁵⁷

Humanization and sequence optimization of 6B8

Humanization was carried out using the M-13-based Fab expression system methods described by Wu et al.⁵⁸ Libraries for the light chain and heavy chain were designed individually, in which selected framework positions contained the amino acid residue from mouse or from the chosen human germ-line template, and the selected CDR positions were subjected to saturation mutagenesis using the NNK codon or to custom mutagenesis using unique mixtures of codons. A combinatorial Fab library of variants was expressed in *E. coli* and screened with an ELISA for IL23 binding to determine which variants maintained a binding affinity equivalent to or greater than the chimera. Fabs showing maintained binding were further screened on a ProteOn XPR36 biosensor (Bio Rad). The off-rate and affinity were used to rank the candidates from the humanization

libraries. Favored residues in the library positions were determined by >80% prevalence within the confirmed hits. Sequences were analyzed for the percentage of human residues in the framework regions and for potential immunogenicity using the Treg adjusted scores from the EpiVax Epimatrix in silico immunogenicity prediction program.⁵⁹ IgG1 antibodies for the selected humanized and optimized clones were expressed initially in HEK293 cells transiently and then in NS0 cells as stable transfectants and purified using standard methods with modifications.⁶⁰⁻⁶² The purified samples were then submitted for biophysical profiling, functional testing, and other studies.

Mouse splenocyte assay (MSA)

The ability of anti-human IL23 antibodies to inhibit the induction of mouse IL17 by either human or cynomolgus recombinant IL23 at the EC80 (7.5 ng/ml and 1.5 ng/ml respectively) was assessed in mouse splenocyte cultures.⁶³ Mononuclear cells from a single mouse spleen (female C57BL/6; JAX) were isolated, washed, counted, and re-suspended to 4×10^6 cells/ml in medium. Recombinant mouse IL2 (R&D Systems) was added to the cells at 20 ng/mL. The antibodies were pre-incubated with IL23, then the mixture was added to the cells, and the test plates were incubated at 37°C with 5% CO₂-humidified air for 48 h. Mouse IL17 levels in the supernatant were determined using the Quantikine® Mouse IL17 Immunoassay according to the manufacturer's instructions (R&D Systems).

In vivo efficacy of anti-human IL23 antibodies in IL23-induced skin inflammation

Mice were given vehicle or 1 mg/kg antibody (i.p.). One hour later, recombinant human IL23 was injected into the skin of the mouse ear for 4 consecutive days. Twenty-four hours after the last IL23 injection, the ear thickness was measured, and the ear tissue was harvested and snap frozen in liquid nitrogen. The tissue was homogenized in Hank's Balanced Salt Solution containing 0.1% Triton-X and SigmaFast protease inhibitor (Sigma) using MPBio Fast-prep lysing matrix A tubes. The homogenized samples were centrifuged at $10,000 \times g$ for 10 minutes, and the supernatant was collected and assayed for mouse IL17 and IL22 using the Quantikine → Mouse Immunoassay according to the manufacturer's instructions (R&D Systems).

Biophysical profiling

Analytical ultracentrifugation (AUC)

All of the AUC experiments were conducted on a Beckman XLI analytical ultracentrifuge (Beckman Coulter, Inc.). The sedimentation velocity experiments were conducted at 40,000 rpm and 20°C. Experiments were conducted in a pH 6.0 buffer containing 20 mM Citrate and 115 mM NaCl. Proteins were detected by the absorbance at 280 nm and were analyzed using the continuous c(S) model in SedFit version 12.1c.⁶⁴

Differential scanning calorimetry

The thermal unfolding and aggregation of sequence-optimized anti-human IL23A IgGs at 1 mg/ml in 20 mM sodium

citrate, 115 mM sodium chloride, pH 6.0 were monitored from 25°C to 110°C at a scan rate of 60°C/h via an automated capillary differential scanning calorimetry (MicroCal, LLC). The data were analyzed using Origin 7.0 software (Origin-Lab). All thermograms were baseline-corrected and fitted using the 2-state model in Origin to obtain the apparent midpoint temperatures (T_m) for unfolding.

Solubility determination

The sequence-optimized antibodies were concentrated from 10 mg/ml to 120 mg/ml using Amicon ultracentrifugal 15 mL filters with a molecular weight cut-off of 50 kDa (EMD Millipore). After concentration, the actual solution concentrations were determined by the absorbance at A280 nm of a sample diluted to < 40 mg/ml, using a UV/VIS Nanodrop 8000 (Thermo Scientific). The homogeneity of the concentrated antibody samples was analyzed by AUC as described above.

Capillary electrophoresis

Capillary electrophoresis (CE) was used for the net charge measurements using a ProteomeLab™ PA800 (Beckman Coulter) instrument equipped with an ultraviolet (UV) absorbance detector with a working wavelength of 214 nm. Temperature was held at 20°C. An eCap amine capillary with an inner diameter of 50 μm (Beckman Coulter) and a total capillary length of 60 cm was used. Capillary length from injection to detector was 50 cm. Protein samples were prepared at a concentration of 1 mg/ml in 10 mM acetate, 50 mM KCl, pH 5.0 buffer and were injected immediately after the injection of an electroosmotic flow (EOF) marker using hydrodynamic injection (0.5 psi for 5 seconds). 0.005% dimethylformamide (DMF) (Sigma) in 10 mM acetate, 50 mM KCl, pH 5.0 buffer was used as EOF marker with detection at 214 nm. Each sample was run at 3 constant current conditions (10, 14 and 18 μA) in 10 mM acetate, 50 mM KCl, pH 5.0 buffer, migration times of the EOF marker and sample were obtained and utilized to calculate their velocities. The electric field was calculated based on current applied, cross-sectional area of the capillary and conductance of the buffer. The apparent electrophoretic mobilities for the EOF and the sample were obtained as the slope of a linear relationship between their respective velocities and the electric field. Subtracting the apparent mobility for EOF from apparent mobility of the sample gives the mobility of the protein (μ_p), corrected for electro-endosmosis.^{65,66} The software program Zutilities was used to calculate apparent valence, z^* , using μ_p from CE, and the diffusion coefficient (D) and hydrodynamic (stokes, R_s) radius determined from sedimentation velocity experiments via Beckman Coulter ProteomeLab™ XL-I using standard protocols described elsewhere.^{65,67} Using Zutilities, apparent valence (z^*) was converted to valence (z) with input of ionic strength of solvent as 50 mM and hydrodynamic radius of the chloride ion (counter ion) as 0.122 nm.

Serum interference

The interaction of antibodies with human IL23 in 1 × kinetic buffer or human serum (Sigma, St. Louis, MO) was analyzed on

an Octet QK (ForteBio) instrument equipped with streptavidin (SA) biosensor tips (ForteBio). The sensors were coated with biotinylated human IL23, and then were dipped in human serum to establish a baseline for binding in serum before analyzing the interaction of BI 655066 with human IL23. The response of the binding sensorgrams in 1× kinetic buffer and human serum at different association time points (60 sec, 120 sec, and 240 sec) were compared to determine if the antibodies bound to off-target molecules present in human serum.

Molecular affinity of human IL23 for BI 655066

A ProteOn XPR36 biosensor (Bio Rad) was used to measure the binding kinetics of human IL23 for the sequence-optimized antibodies. Goat anti-human IgG gamma Fc specific (GAHA) (Invitrogen) was immobilized to the dextran matrix of a GLM sensor chip (Bio Rad, Hercules, CA) along 6 horizontal channels using an amine coupling kit (Bio Rad), at a surface density of 8000-10,000 resonance units (RU), according to the manufacturer's instructions. BI 655066 was captured on the GAHA surface along 5 vertical channels at a surface density of ~200 RU. The last vertical channel was used as a column reference to remove bulk shift. The binding kinetics of human IL23 for each antibody was determined by the global fitting of duplicate injections of human IL23 at 5 dilutions (10, 5.0, 2.5, 1.25, 0.625, and 0 nM). The collected binding sensorgrams of human IL23 at 5 concentrations with duplicates were double referenced using an inactive channel / inter-spot reference and an extraction buffer reference. The referenced sensorgrams were fit to a 1:1 Langmuir binding model to determine the association rate (k_{on}), dissociation rate (k_{off}), and dissociation constant (K_d).

Epitope mapping

Identification of peptides and deuterium exchange experiments

Protein alone (5 nM) or protein/antibody complex (5 nM/50 nM) was mixed with an excess volume of buffer (50 mM phosphate-buffered saline (PBS) in H₂O) or deuterated buffer (50 mM PBS in D₂O). After 100 seconds at room temperature, Urea/TCEP was added and mixed. After 1 minute, pepsin or protease XIII P was added, and the entire volume was immediately transferred to a 96-well plate, at 4°C. After 5 minutes, 50 µl of this solution was injected onto a Phenomenex Jupiter C5 column. The peptides were eluted from the column with a gradient of Mobile Phase A (water/acetonitrile/formic acid, 99/1/0.1) and Mobile Phase B (acetonitrile/water/formic acid, 95/5/0.1), as follows: Time = 0 min (3%B), Time = 2.2 min (3%B), Time = 10.1 min (90%B), Time = 12.0 min (90%B), and Time = 12.1 min (3%B). Three replicates were done for both the control (IL23 alone) and the experiment (IL23 with antibody). The chromatographic effluent was directed into a Thermo Orbitrap Velos mass spectrometer, and monitored in-line by electrospray ionization (ESI). For peptide identification experiments, data were acquired for 12 minutes (3-minute delay start time), in full-scan mode at 30,000 resolution, followed by 7 ion trap data dependent scans (collision-induced dissociation, CID). Peptides were identified using the fragmentation data and the

program Proteome Discoverer (Thermo Scientific). For the deuterium exchange experiments, data were acquired for 12 minutes (3 minute delay start time), in full-scan mode at 60,000 resolution. Data were analyzed using the PepMap program (Thermo Scientific).

Cynomolgus monkey PK analysis

Intravenous and subcutaneous PK of BI 655066 were evaluated in cynomolgus monkeys. The studies were approved by Boehringer Ingelheim Pharmaceuticals, Inc. Institutional Animal Care and Use Committee, and were in compliance with the US Department of Agriculture Animal Welfare Act (9CFR Parts 1, 2, and 3). BI 655066 was administered either by subcutaneous injection to the middle interscapular region or intravenously as a 10-minute infusion into the right saphenous vein. The serum concentrations of BI 655066 were determined using a validated, antigen-capture ELISA. Briefly, biotinylated IL23 was immobilized onto streptavidin-coated Nunc MaxiSorp 96-well plates (Affimetrix eBioscience). The plates were washed, then blocked with PBS and 2% BSA (w/v). Matrix reference standards, quality control, and test samples were then diluted to a final concentration of 5% monkey serum and transferred to the blocked plate. The plates were washed, then 0.05 µg/ml goat anti-human IgG-HRP (Southern Biotech) was added. The plates were washed again, and the BioF_x (SurModics) substrate TMBW was added. The plates were allowed to develop for ~5 minutes at room temperature, then the BioF_x liquid stop solution for TMB substrate (0.2 M H₂SO₄) was added, and the plates were analyzed on a SpectraMax (Molecular Devices) M5 Plate Reader at OD 450 nM. Concentrations were derived from a standard curve, obtained by plotting the 450 OD signal intensity versus the concentration of known samples, then fitting the log-log curve using Softmax Pro software (Molecular Devices). Non-compartmental PK analysis was performed using WinNonlin software (v. 5.3, Pharsight Corporation). To estimate the terminal half-life ($t_{1/2}$), the area under the serum concentration-vs.-time curve to the last quantifiable time point (AUC_{0-t}) was calculated using the linear trapezoidal method and extrapolated to time infinity (AUC_{inf}) using log-linear regression of the terminal portion of the curves. The elimination rate constant (k_{el}) was determined by least-squares regression of the log-transformed concentration data using the terminal phase, identified by obtaining measurements between days 1 and 42, and $t_{1/2}$ was equal to $\ln 2/k_{el}$.

Disclosure of Potential Conflicts of Interest

No potential conflicts of interest were disclosed.

Acknowledgments

The authors acknowledge the following individuals for their contributions in reviewing the manuscript or providing technical expertise: Robert Copenhaver, Kathleen Last-Barney, Hua Li, and Danlin Yang. We thank Jeanne Magram for support regarding the therapeutic concept. We thank

Gerald Nabozny for help with the mouse in vivo experiments and Raj Nagaraja for help in the monkey pharmacokinetic studies.

Supplemental Material

Supplemental data for this article can be accessed on the publisher's website.

References

- Baeten DL, Kuchroo VK. How Cytokine networks fuel inflammation: interleukin-17 and a tale of two autoimmune diseases. *Nat Med* 2013; 19:824-5; PMID:23836225; <http://dx.doi.org/10.1038/nm.3268>
- Gaffen SL, Jain R, Garg AV, Cua DJ. The IL-23-IL-17 immune axis: from mechanisms to therapeutic testing. *Nat Rev Immunol* 2014; 14:585-600; PMID:25145755; <http://dx.doi.org/10.1038/nri3707>
- Toussiot E. The IL23/Th17 pathway as a therapeutic target in chronic inflammatory diseases. *Inflamm Allergy Drug Targets* 2012; 11:159-68; PMID:22280236; <http://dx.doi.org/10.2174/187152812800392805>
- Elmaagacli AH, Koldehoff M, Landt O, Beelen DW. Relation of an interleukin-23 receptor gene polymorphism to graft-versus-host disease after hematopoietic cell transplantation. *Bone Marrow Transplant* 2008; 41:821-6; PMID:18209723; <http://dx.doi.org/10.1038/sj.bmt.1705980>
- Capon F, Di MP, Szaub J, Prescott NJ, Dunster C, Baumber L, Timms K, Gutin A, Abkevic V, Burden AD, et al. Sequence variants in the genes for the interleukin-23 receptor (IL23R) and its ligand (IL12B) confer protection against psoriasis. *Hum Genet* 2007; 122:201-6; PMID:17587057; <http://dx.doi.org/10.1007/s00439-007-0397-0>
- McGovern D, Powrie F. The IL23 axis plays a key role in the pathogenesis of IBD. *Gut* 2007; 56:1333-6; PMID:17872562; <http://dx.doi.org/10.1136/gut.2006.115402>
- Tausend W, Downing C, Tying S. Systematic review of interleukin-12, interleukin-17, and interleukin-23 pathway inhibitors for the treatment of moderate-to-severe chronic plaque psoriasis: ustekinumab, briakinumab, tildrakizumab, guselkumab, secukinumab, ixekicimab, and brodalumab. *J Cutan Med Surg* 2014; 18:156-69; PMID:24800703
- McGeachy MJ, Chen Y, Tato CM, Laurence A, Joyce-Shaikh B, Blumenschein WM, McClanahan TK, O'Shea JJ, Cua DJ. The interleukin 23 receptor is essential for the terminal differentiation of interleukin 17-producing effector T helper cells in vivo. *Nat Immunol* 2009; 10:314-24; PMID:19182808; <http://dx.doi.org/10.1038/ni.1698>
- Hsieh CS, Macatonia SE, Tripp CS, Wolf SF, O'Garra A, Murphy KM. Development of TH1 CD4+ T cells through IL-12 produced by Listeria-induced macrophages. *Science* 1993; 260:547-9; PMID:8097338; <http://dx.doi.org/10.1126/science.8097338>
- McGeachy MJ, Cua DJ. The link between IL-23 and Th17 cell-mediated immune pathologies. *Semin Immunol* 2007; 19:372-6; PMID:18319054; <http://dx.doi.org/10.1016/j.smim.2007.10.012>
- Ghoreschi K, Laurence A, Yang XP, Tato CM, McGeachy MJ, Konkel JE, Ramos HL, Wei L, Davidson TS, Bouladoux N, et al. Generation of pathogenic T(H)17 cells in the absence of TGF-beta signalling. *Nature* 2010; 467:967-71; PMID:20962846; <http://dx.doi.org/10.1038/nature09447>
- Teunissen MB, Munneke JM, Bernink JH, Spuls PI, Res PC, Te VA, Cheuk S, Brouwer MW, Menting SP, Eidsmo L, et al. Composition of innate lymphoid cell subsets in the human skin: enrichment of NCR(+) ILC3 in lesional skin and blood of psoriasis patients. *J Invest Dermatol* 2014; 134:2351-60; PMID:24658504; <http://dx.doi.org/10.1038/jid.2014.146>
- Villanova F, Flutter B, Tosi I, Grys K, Sreeneebus H, Perera GK, Chapman A, Smith CH, Di MP, Nestle FO. Characterization of innate lymphoid cells in human skin and blood demonstrates increase of NKp44+ ILC3 in psoriasis. *J Invest Dermatol* 2014; 134:984-91; PMID:24352038; <http://dx.doi.org/10.1038/jid.2013.477>
- Harrington LE, Hatton RD, Mangan PR, Turner H, Murphy TL, Murphy KM, Weaver CT. Interleukin 17-producing CD4+ effector T cells develop via a lineage distinct from the T helper type 1 and 2 lineages. *Nat Immunol* 2005; 6:1123-32; PMID:16200070; <http://dx.doi.org/10.1038/ni1254>
- Langrish CL, Chen Y, Blumenschein WM, Mattson J, Basham B, Sedgwick JD, McClanahan T, Kastelein RA, Cua DJ. IL-23 drives a pathogenic T cell population that induces autoimmune inflammation. *J Exp Med* 2005; 201:233-40; PMID:15657292; <http://dx.doi.org/10.1084/jem.20041257>
- Park H, Li Z, Yang XO, Chang SH, Nurieva R, Wang YH, Wang Y, Hood L, Zhu Z, Tian Q, et al. A distinct lineage of CD4 T cells regulates tissue inflammation by producing interleukin 17. *Nat Immunol* 2005; 6:1133-41; PMID:16200068
- Chung Y, Chang SH, Martinez GJ, Yang XO, Nurieva R, Kang HS, Ma L, Watowich SS, Jetten AM, Tian Q, et al. Critical regulation of early Th17 cell differentiation by interleukin-1 signalling. *Immunity* 2009; 30:576-87; PMID:19362022
- Abdi K, Singh NJ, Spooner E, Kessler BM, Radaev S, Lantz L, Xiao TS, Matzinger P, Sun PD, Ploegh HL. Free IL-12p40 monomer is a polyfunctional adaptor for generating novel IL-12-like heterodimers extracellularly. *J Immunol* 2014; 192:6028-36; PMID:24821971
- Paunovic V, Carroll HP, Vandenbroeck K, Gadina M. Signalling, inflammation and arthritis: crossed signals: the role of interleukin (IL)-12, -17, -23 and -27 in autoimmunity. *Rheumatology(Oxford)* 2008; 47:771-6; PMID:18238793
- Brand S. Crohn's disease: Th1, Th17 or both? The change of a paradigm: new immunological and genetic insights implicate Th17 cells in the pathogenesis of Crohn's disease. *Gut* 2009; 58:1152-67; PMID:19592695
- Zhou L, Littman DR. Transcriptional regulatory networks in Th17 cell differentiation. *Curr Opin Immunol* 2009; 21:146-52
- Yang XP, Ghoreschi K, Steward-Tharp SM, Rodriguez-Canales J, Zhu J, Grainger JR, Hirahara K, Sun HW, Wei L, Vahedi G, et al. Opposing regulation of the locus encoding IL-17 through direct, reciprocal actions of STAT3 and STAT5. *Nat Immunol* 2011; 12:247-54; PMID:21278738
- Krueger J, Ferris LK, Menter A, Wagner F, White A, Visvanatha S, Lalovic V, Aslanyan S, Hall D, Soinger A, et al. Anti-IL-23A monoclonal antibody BI 655066 for treatment of moderate-to-severe psoriasis: Safety, efficacy, pharmacokinetics and biomarker results of a single-rising-dose, randomised, double-blind, placebo-controlled trial. *J All Clin Immunol* 2014 (in press)
- Parham C, Chirica M, Timans J, Vaisberg E, Travis M, Cheung J, Pflanz S, Zhang R, Singh KP, Vega F, et al. A receptor for the heterodimeric cytokine IL-23 is composed of IL-12Rbeta1 and a novel cytokine receptor subunit, IL-23R. *J Immunol* 2002; 168:5699-708; PMID:12023369
- Jones PT, Dear PH, Foote J, Neuberger MS, Winter G. Replacing the complementarity-determining regions in a human antibody with those from a mouse. *Nature* 1986; 321:522-5; PMID:3713831
- Hale G, Dyer MJ, Clark MR, Phillips JM, Marcus R, Riechmann L, Winter G, Waldmann H. Remission induction in non-Hodgkin lymphoma with reshaped human monoclonal antibody CAMPATH-1H. *Lancet* 1988; 2:1394-9; PMID:2904526
- Almagro JC, Fransson J. Humanization of antibodies. *Front Biosci* 2008; 13:1619-33; PMID:17981654
- Xu D, Alegre ML, Varga SS, Rothermel AL, Collins AM, Pulito VL, Hanna LS, Dolan KP, Parren PW, Bluestone JA, et al. In vitro characterization of five humanized OKT3 effector function variant antibodies. *Cell Immunol* 2000; 200:16-26; PMID:10716879
- Laue TM, Stafford WF, III. Modern applications of analytical ultracentrifugation. *Annu Rev Biophys Biomol Struct* 1999; 28:75-100; PMID:10410796
- Torrens F. Valence topological charge-transfer indices for dipole moments. *Mol Divers* 2004; 8:365-70; PMID:15612640
- Yadav S, Laue TM, Kalonia DS, Singh SN, Shire SJ. The influence of charge distribution on self-association and viscosity behavior of monoclonal antibody solutions. *Mol Pharm* 2012; 9:791-802; PMID:22352470; <http://dx.doi.org/10.1021/mp200566k>
- Clementi N, Mancini N, Criscuolo E, Cappelletti F, Clementi M, Burioni R. Epitope mapping by epitope excision, hydrogen/deuterium exchange, and peptide-panning techniques combined with in silico analysis. *Methods Mol Biol* 2014; 1131:427-46; PMID:24515481; http://dx.doi.org/10.1007/978-1-62703-992-5_26
- Ling J, Zhou H, Jiao Q, Davis HM. Interspecies scaling of therapeutic monoclonal antibodies: initial look. *J Clin Pharmacol* 2009; 49:1382-402; PMID:19837907; <http://dx.doi.org/10.1177/0091270009337134>
- Griffiths CE, Strober BE, van de Kerkhof P, Ho V, Fidelus-Gort R, Yeilding N, Guzzo C, Xia Y, Zhou B, Li S, et al. Comparison of ustekinumab and etanercept for moderate-to-severe psoriasis. *N Engl J Med* 2010; 362:118-28; PMID:20071701; <http://dx.doi.org/10.1056/NEJMoa0810652>
- Ouyang W, Kolls JK, Zheng Y. The biological functions of T helper 17 cell effector cytokines in inflammation. *Immunity* 2008; 28:454-67; PMID:18400188; <http://dx.doi.org/10.1016/j.immuni.2008.03.004>
- Sherlock JP, Joyce-Shaikh B, Turner SP, Chao CC, Sath M, Grein J, Gorman DM, Bowman EP, McClanahan TK, Yearley JH, et al. IL-23 induces spondyloarthritis by acting on ROR-gamma+ CD3+CD4-CD8- entheseal resident T cells. *Nat Med* 2012; 18:1069-76; PMID:22772566; <http://dx.doi.org/10.1038/nm.2817>
- Witte E, Witte K, Warsawska K, Sabat R, Wolk K. Interleukin-22: a cytokine produced by T, NK and NKT cell subsets, with importance in the innate immune defense and tissue protection. *Cytokine Growth Factor Rev* 2010; 21:365-79; PMID:20870448; <http://dx.doi.org/10.1016/j.cytogr.2010.08.002>
- Paes AH, Bakker A, Soe-Agnie CJ. Impact of dosage frequency on patient compliance. *Diabetes Care* 1997; 20:1512-7; PMID:9314626; <http://dx.doi.org/10.2337/diacare.20.10.1512>
- Lee EC, Liang Q, Ali H, Bayliss L, Beasley A, Bloomfield-Gerdes T, Bonoli L, Brown R, Campbell J, Carpenter A, et al. Complete humanization of the mouse immunoglobulin loci enables efficient therapeutic antibody discovery. *Nat Biotechnol* 2014; 32:356-63; PMID:24633243; <http://dx.doi.org/10.1038/nbt.2825>
- Reichert JM. Antibodies to watch in 2014. *MAbs* 2014; 6:5-14; PMID:24284914; <http://dx.doi.org/10.4161/mabs.27333>
- Rajewsky K. Clonal selection and learning in the antibody system. *Nature* 1996; 381:751-8; PMID:8657279; <http://dx.doi.org/10.1038/381751a0>
- Takemori T, Kaji T, Takahashi Y, Shimoda M, Rajewsky K. Generation of memory B cells inside and outside germinal centers. *Eur J Immunol* 2014; 44:1258-64;

- PMID:24610726; <http://dx.doi.org/10.1002/cji.201343716>
43. De Groot AS, Moise L, McMurry JA, Wambre E, Van OL, Moingeon P, Scott DW, Martin W. Activation of natural regulatory T cells by IgG Fc-derived peptide "Tregitopes." *Blood* 2008; 112:3303-11; PMID:18660382; <http://dx.doi.org/10.1182/blood-2008-02-138073>
 44. Rosok MJ, Yelton DE, Harris LJ, Bajorath J, Hellstrom KE, Hellstrom I, Cruz GA, Kristensson K, Lin H, Huse WD, et al. A combinatorial library strategy for the rapid humanization of anticarcinoma BR96 Fab. *J Biol Chem* 1996; 271:22611-8; PMID:8798431; <http://dx.doi.org/10.1074/jbc.271.37.22611>
 45. Waldmann H. Human monoclonal antibodies: the residual challenge of antibody immunogenicity. *Methods Mol Biol* 2014; 1060:1-8; PMID:24037833; http://dx.doi.org/10.1007/978-1-62703-586-6_1
 46. Ewert S, Huber T, Honegger A, Pluckthun A. Biophysical properties of human antibody variable domains. *J Mol Biol* 2003; 325:531-53; PMID:12498801; [http://dx.doi.org/10.1016/S0022-2836\(02\)01237-8](http://dx.doi.org/10.1016/S0022-2836(02)01237-8)
 47. Garber E, Demarest SJ. A broad range of Fab stabilities within a host of therapeutic IgGs. *Biochem Biophys Res Commun* 2007; 355:751-7; PMID:17321501; <http://dx.doi.org/10.1016/j.bbrc.2007.02.042>
 48. Kuramochi T, Igawa T, Tsunoda H, Hattori K. Humanization and simultaneous optimization of monoclonal antibody. *Methods Mol Biol* 2014; 1060:123-37; PMID:24037839; http://dx.doi.org/10.1007/978-1-62703-586-6_7
 49. Rosenberg AS. Effects of protein aggregates: an immunologic perspective. *Amer Assoc Pharm Sci J* 2006; 8: E501-E7
 50. De Groot AS, Scott DW. Immunogenicity of protein therapeutics. *Trends Immunol* 2007; 28:482-90; PMID:17964218; <http://dx.doi.org/10.1016/j.it.2007.07.011>
 51. Joshi V, Shivach T, Kumar V, Yadav N, Rathore A. Avoiding antibody aggregation during processing: Establishing hold times. *Biotechnol J* 2014; 9(9):1195-205; PMID:24753430
 52. Manning MC, Chou DK, Murphy BM, Payne RW, Katayama DS. Stability of protein pharmaceuticals: an update. *Pharm Res* 2010; 27:544-75; PMID:20143256; <http://dx.doi.org/10.1007/s11095-009-0045-6>
 53. He F, Woods CE, Trilisky E, Bower KM, Litowski JR, Kerwin BA, Becker GW, Narhi LO, Razinkov VI. Screening of monoclonal antibody formulations based on high-throughput thermostability and viscosity measurements: design of experiment and statistical analysis. *J Pharm Sci* 2011; 100:1330-40; PMID:24081468; <http://dx.doi.org/10.1002/jps.22384>
 54. Lobo ED, Hansen RJ, Balthasar JP. Antibody pharmacokinetics and pharmacodynamics. *J Pharm Sci* 2004; 93:2645-68; PMID:15389672; <http://dx.doi.org/10.1002/jps.20178>
 55. He R, Shepard LW, Chen J, Pan ZK, Ye RD. Serum amyloid A is an endogenous ligand that differentially induces IL-12 and IL-23. *J Immunol* 2006; 177:4072-9; PMID:16951371; <http://dx.doi.org/10.4049/jimmunol.177.6.4072>
 56. Harlow E, Lane D. *Using Antibodies: A Laboratory Manual*. Plainview, NY: Cold Spring Harbor Laboratory Press; 1999
 57. Welschof M, Krauss J. *Recombinant Antibodies for Cancer Therapy: Methods and Protocols*. Totowa, NJ: Humana Press; 2003
 58. Wu H, An LL. Tailoring kinetics of antibodies using focused combinatorial libraries. *Methods Mol Biol* 2003; 207:213-33; PMID:12412477
 59. De Groot AS, Martin W. Reducing risk, improving outcomes: bioengineering less immunogenic protein therapeutics. *Clin Immunol* 2009; 131:189-201; PMID:19269256; <http://dx.doi.org/10.1016/j.clim.2009.01.009>
 60. Schmidt M, Hafner M, Frech C. Modeling of salt and pH gradient elution in ion-exchange chromatography. *J Sep Sci* 2014; 37:5-13; PMID:24415551; <http://dx.doi.org/10.1002/jssc.201301007>
 61. Sheeley DM, Merrill BM, Taylor LC. Characterization of monoclonal antibody glycosylation: comparison of expression systems and identification of terminal alpha-linked galactose. *Anal Biochem* 1997; 247:102-10; PMID:9126378; <http://dx.doi.org/10.1006/abio.1997.2036>
 62. Brown NL, Bottomley SP, Gore MG. Affinity purification of human IgG using immobilised, mutated immunoglobulin-binding domains from protein A of *Staphylococcus aureus*. *Biochem Soc Trans* 1998; 26: S249; PMID:9765968
 63. Aggarwal S, Ghilardi N, Xie MH, de Sauvage FJ, Gurney AL. Interleukin-23 promotes a distinct CD4 T cell activation state characterized by the production of interleukin-17. *J Biol Chem* 2003; 278:1910-4; PMID:12417590; <http://dx.doi.org/10.1074/jbc.M207577200>
 64. Schuck P. Size-distribution analysis of macromolecules by sedimentation velocity ultracentrifugation and lamm equation modeling. *Biophys J* 2000; 78:1606-19; PMID:10692345; [http://dx.doi.org/10.1016/S0006-3495\(00\)76713-0](http://dx.doi.org/10.1016/S0006-3495(00)76713-0)
 65. Chase S, Laue TM. The determination of protein valence by capillary electrophoresis. *PACE Setter* 2008; 12(1):1-5
 66. Adamson NJ, Reynolds EC. Rules relating electrophoretic mobility, charge and molecular size of peptides and proteins. *J Chromatogr B Biomed Sci Appl* 1997; 699:133-47; PMID:9392373; [http://dx.doi.org/10.1016/S0378-4347\(97\)00202-8](http://dx.doi.org/10.1016/S0378-4347(97)00202-8)
 67. Brown PH, Schuck P. Macromolecular size-and-shape distributions by sedimentation velocity analytical ultracentrifugation. *Biophys J* 2006; 90:4651-61; PMID:16565040; <http://dx.doi.org/10.1529/biophysj.106.081372>